

# Sparse Tensor Additive Regression

Botao Hao\*, Boxiang Wang<sup>†</sup>, Pengyuan Wang<sup>‡</sup>,  
Jingfei Zhang<sup>§</sup>, Jian Yang<sup>¶</sup>, Will Wei Sun<sup>||</sup>

## Abstract

Tensors are becoming prevalent in modern applications such as medical imaging and digital marketing. In this paper, we propose a sparse tensor additive regression (STAR) that models a scalar response as a flexible nonparametric function of tensor covariates. The proposed model effectively exploits the sparse and low-rank structures in the tensor additive regression. We formulate the parameter estimation as a non-convex optimization problem, and propose an efficient penalized alternating minimization algorithm. We establish a non-asymptotic error bound for the estimator obtained from each iteration of the proposed algorithm, which reveals an interplay between the optimization error and the statistical rate of convergence. We demonstrate the efficacy of STAR through extensive comparative simulation studies, and an application to the click-through-rate prediction in online advertising.

KEY WORDS: Additive models; low-rank tensor; non-asymptotic analysis; non-convex optimization; tensor regression.

---

\*Ph.D student, Department of Statistics, Purdue University, West Lafayette, IN 47906. E-mail: hao22@purdue.edu.

<sup>†</sup>Assistant Professor, Department of Statistics and Actuarial Science, The University of Iowa, Iowa City, IA 52242.

E-mail: boxiang-wang@uiowa.edu.

<sup>‡</sup>Assistant Professor, Department of Marketing, University of Georgia, Athens, GA 30602. E-mail: pengyuan@uga.edu.

<sup>§</sup>Assistant Professor, Department of Management Science, University of Miami, Coral Gables, FL 33146. Email: ezhang@bus.miami.edu.

<sup>¶</sup>Senior Director, Yahoo Research, Sunnyvale, CA 94089. E-mail: jianyang@oath.com.

<sup>||</sup>Assistant Professor, Department of Management Science, University of Miami, Coral Gables, FL 33146. Email: wsun@bus.miami.edu.

# 1 Introduction

Tensor data have recently become popular in a wide range of applications such as medical imaging (Zhou et al., 2013; Li and Zhang, 2017; Sun and Li, 2017), digital marketing (Zhe et al., 2016; Sun et al., 2017), video processing (Guo et al., 2012), and social network analysis (Park and Chu, 2009; Hoff, 2015), among many others. In such applications, a fundamental statistical tool is *tensor regression*, a modern high-dimensional regression method that relates a scalar response to tensor covariates. For example, in neuroimaging analysis, an important objective is to predict clinical outcomes using subjects’ brain imaging data. This can be formulated as a tensor regression problem by treating the clinical outcomes as the response and the brain images as the tensor covariates. Another example is in the study of how advertisement placement affect users’ clicking behavior in online advertising. This again can be formulated as a tensor regression problem by treating the daily overall click-through rate (CTR) as the response and the tensor that summarizes the impressions (i.e., view counts) of different advertisements on different devices (e.g., phone, computer, etc.) as the covariate. In Section 6, we consider such an online advertising application.

Denote  $y_i$  as a scalar response and  $\mathcal{X}_i \in \mathbb{R}^{p_1 \times p_2 \times \dots \times p_m}$  as an  $m$ -way tensor covariate,  $i = 1, 2, \dots, n$ . A general tensor regression model can be formulated as

$$y_i = \mathcal{T}^*(\mathcal{X}_i) + \epsilon_i, \quad i = 1, 2, \dots, n,$$

where  $\mathcal{T}^*(\cdot) : \mathbb{R}^{p_1 \times p_2 \times \dots \times p_m} \rightarrow \mathbb{R}$  is an unknown regression function,  $\{\epsilon_i\}_{i=1}^n$  are scalar observation noises. Many existing methods assumed a linear relationship between the response and the tensor covariates by considering  $\mathcal{T}^*(\mathcal{X}_i) = \langle \mathcal{B}, \mathcal{X}_i \rangle$  for some low-rank tensor coefficient  $\mathcal{B}$  (Zhou et al., 2013; Rabusseau and Kadri, 2016; Yu and Liu, 2016; Guhaniyogi et al., 2017; Raskutti et al., 2019). In spite of its simplicity, the linear assumption could be restrictive and difficult to satisfy in real applications. Consider the online advertising data in Section 6 as an example. Figure 1 shows the marginal relationship between the overall CTR and the impressions of an advertisement delivered on phone, tablet, and PC, respectively. It is clear that the relationship between the response (i.e., the overall CTR) and the covariate (i.e., impressions across three devices) departs notably from the linearity assumption. A few work considered more flexible tensor regressions by treating  $\mathcal{T}^*(\cdot)$  as a nonparametric function (Suzuki et al., 2016; Kanagawa et al., 2016). In particular, Suzuki et al. (2016) proposed a general nonlinear model where the true function  $\mathcal{T}^*(\cdot)$  is consisted of components from a reproducing kernel Hilbert space, and used an alternating minimization estimation procedure; Kanagawa et al. (2016) considered a Bayesian approach that employed a Gaussian process prior in learning the nonparametric function  $\mathcal{T}^*(\cdot)$  on the reproducing kernel

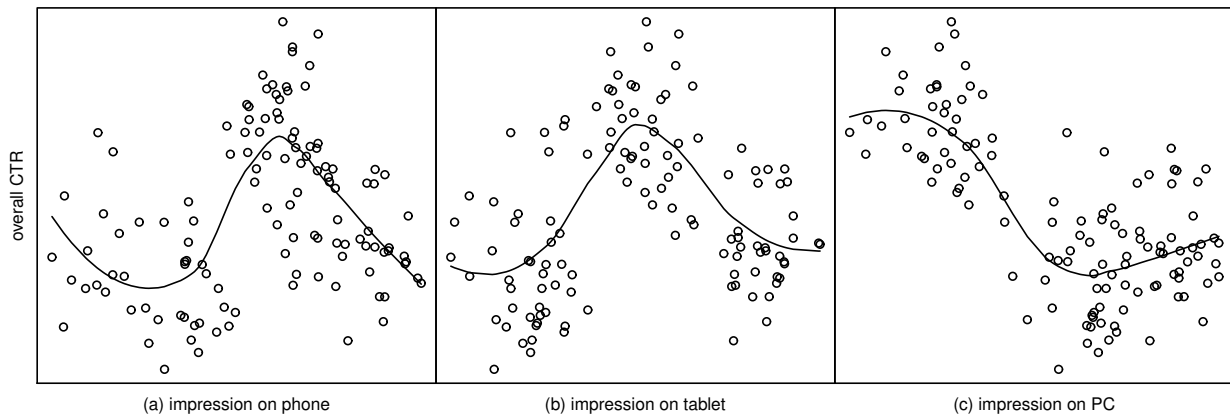


**Figure 1.** The overall click-through rate v.s. the impression of a certain advertisement that is delivered on phone (left plot), tablet (middle plot), and PC (right plot), respectively. The black solid curves are the fitted locally weighted scatter-plot smoother (LOESS) curves.

Hilbert space. One serious limitation of both work is that they assume that the tensor covariates are *exact low-rank*. This assumption is difficult to satisfy in practice, as most tensor covariates are not exact low-rank. When the tensor covariates are not exact low-rank, the performance of these two methods deteriorates dramatically; see Section 5.2 for more details. In addition, the Gaussian process approach is computationally very expensive, which severely limits its application in problems with high-dimensional tensor covariates.

In this paper, we develop a flexible and computationally feasible tensor regression framework, which accommodates the nonlinear relationship between the response and the tensor covariate, and is highly interpretable. Specifically, for an  $m$ -way tensor covariate  $\mathcal{X}_i \in \mathbb{R}^{p_1 \times \dots \times p_m}$ , we consider a sparse tensor additive regression (STAR) model with

$$\mathcal{T}^*(\mathcal{X}_i) = \sum_{j_1=1}^{p_1} \cdots \sum_{j_m=1}^{p_m} f_{j_1 \dots j_m}^*([\mathcal{X}_i]_{j_1 \dots j_m}), \quad (1.1)$$

where  $[\mathcal{X}_i]_{j_1 \dots j_m}$  denotes the  $(j_1, \dots, j_m)$ -th element of  $\mathcal{X}_i$ , and  $f_{j_1 \dots j_m}^*(\cdot)$  is a nonparametric additive component belonging to some smooth function class. Approximating the additive component  $f_{j_1 \dots j_m}^*(\cdot)$  using spline series expansions,  $\mathcal{T}^*(\mathcal{X}_i)$  can be simplified to have a compact tensor representation of spline coefficients. To reduce the number of parameters and increase computational efficiency, we assume that the corresponding high-dimensional coefficient tensors have low-rank and group sparsity structures. Both low-rankness and sparsity are commonly used dimension reduction tools in recent tensor models (Li and Zhang, 2017; Sun et al., 2017; Sun and Li, 2017; Hao et al.,

2018; Zhang, 2019; Zhang and Han, 2019). Besides effectively reducing computational cost, the group sparsity structure also significantly improves the model interpretability. For instance, in the online advertising example, when the daily overall CTR is regressed on the impressions of different advertisements on different devices, the group sparsity enables our STAR model to select effective advertisement and device combinations. Such a type of advertisement selection is important for managerial decision making and has been an active research area (Choi et al., 2010; Xu et al., 2016). To efficiently estimate the model, we formulate the parameter estimation as a non-convex optimization and propose a penalized alternating minimization algorithm. By fully exploiting the low-rankness and group sparsity structures, our algorithm may run faster than the tensor linear regression in some experiments. For example, in the online advertising application, our STAR model can reduce the CTR prediction error by 50% while using 10% computational time of the linear or nonlinear tensor regression benchmark models. See Section 6 for more details.

Besides methodological contributions, we also obtain some strong theoretical results for our proposed method. In particular, we first establish a general theory for penalized alternating minimization in the context of tensor additive model. To the best of our knowledge, this is the first statistical-versus-optimization guarantee for the penalized alternating minimization. Previous work mostly focus on either the EM-type update (Wang et al., 2014; Balakrishnan et al., 2017; Hao et al., 2017), or the truncation-based update (Sun et al., 2017). Those techniques are not directly applicable to our scenario; see Section 4.1 for detailed explanations. Next, we derive a non-asymptotic error bound for the estimator from each iteration, which demonstrates the improvement of the estimation error in each update. Finally, we apply this general theory to our STAR estimator with B-spline basis and the group-lasso penalty, and show that the estimation error in the  $(t + 1)$ -th iteration satisfies

$$\mathcal{E}^{(t+1)} \leq \underbrace{\rho^{t+1} \mathcal{E}^{(0)}}_{\text{optimization error}} + \underbrace{\frac{C_1}{1-\rho} n^{-\frac{2\kappa-1}{2\kappa+1}} \log(pd_n)}_{\text{statistical error}},$$

where  $0 < \rho \leq 1/2$  is a contraction parameter,  $\kappa$  is the smoothness parameter of the function class,  $p = \max\{p_1, \dots, p_m\}$ , and  $d_n$  is the number of spline series. The above error bound reveals an interesting interplay between the optimization error and the statistical error. The optimization error decays geometrically with the iteration number  $t$ , while the statistical error remains the same as  $t$  grows. When the tensor covariate is of order one (i.e., a vector covariate), our problem reduces to the vector nonparametric additive model. In that case, our statistical error matches with that from the vector nonparametric additive model in Huang et al. (2010).

## 1.1 Other related work

The problem we consider in our work is fundamentally different from those in tensor decomposition and tensor response regression. As a result, the technical tools involved and the theoretical results are quite different.

Tensor decomposition (Chi and Kolda, 2012; Anandkumar et al., 2014; Yuan and Zhang, 2016; Sun et al., 2017) is an unsupervised learning method that aims to find the best low-rank approximation of a single tensor. In comparison, our STAR model is a supervised learning method that seeks to capture the nonlinear relationship between the response and the tensor covariate. Although the low-rank structure of the tensor coefficient is also employed in our estimation, our objective and the technical tools involved are entirely different from the typical tensor decomposition problem. Additionally, one fundamental difference is that our model works with multiple tensor samples, while tensor decomposition works only with a single tensor. As a result, our error bound is a function of the sample size, which is different from that in tensor decomposition.

Another line of related work considers tensor response regression, where the response is a tensor and the covariates are scalars (Zhu et al., 2009; Li and Zhang, 2017; Sun and Li, 2017). These work also utilized the low-rank and/or sparse structures of the coefficient tensors for dimension reduction. However, tensors are treated as the *response* in tensor response regression, whereas they are treated as a *covariates* in our approach. These are two very different types of models, motivated by different applications. The tensor response regression aims to study the change of the tensor (e.g., the brain image) as the covariate (e.g., disease status) varies. However, the tensor regression model focuses on understanding the change of a scalar outcome (e.g., the overall CTR) with the tensor covariates. As a result, technical tools used for theoretical analysis are also largely different.

## 1.2 Notations and structure

Throughout this article, we denote scalars by lower case characters such as  $x$ , vectors by lower-case bold characters such as  $\mathbf{x}$ , matrices by upper-case bold characters such as  $\mathbf{X}$  and tensors by upper-case script characters such as  $\mathcal{X}$ . Given a vector  $\mathbf{x} \in \mathbb{R}^p$  and a set of indices  $T \subset \{1, \dots, p\}$ , we define  $\mathbf{x}_T$  such that  $x_{T_j} = x_j$  if  $j \in T$  and  $x_{T_j} = 0$ , otherwise. For a square matrix  $\mathbf{A}$ , we denote  $\sigma_{\min}(\mathbf{A})$  and  $\sigma_{\max}(\mathbf{A})$  as its minimum and maximum eigenvalues, respectively. For any function  $f$  on  $[a, b]$ , we define its  $\ell_2(P)$  norm by  $\|f(x)\|_2 = \sqrt{\int_a^b f^2(x)dP(x)}$ . Suppose  $\mathcal{X}, \mathcal{Y} \in \mathbb{R}^{p_1 \times p_2 \times \dots \times p_m}$  are  $m$ -way tensors. We define tensor inner product  $\langle \mathcal{X}, \mathcal{Y} \rangle = \sum_{j_1, \dots, j_m} \mathcal{X}_{j_1 \dots j_m} \mathcal{Y}_{j_1 \dots j_m}$ . The tensor Frobenius norm is defined as  $\|\mathcal{X}\|_F = \sqrt{\sum_{j_1=1}^{p_1} \dots \sum_{j_m=1}^{p_m} \mathcal{X}_{j_1 \dots j_m}^2}$ . The notation  $a \lesssim b$  implies  $a \leq C_1 b$  for some constant  $C_1 > 0$ . For any two sequences  $\{a_n\}_{n=1}^\infty, \{b_n\}_{n=1}^\infty$ , we write  $a_n = \mathcal{O}(b_n)$  if

there exists some positive constant  $C_2$  and sufficiently large  $n$  such that  $a_n \leq C_2 b_n$ . We also write  $a_n \asymp b_n$  if there exist constants  $C_3, C_4 > 0$  such that  $C_3 a_n \leq b_n \leq C_4 a_n$  for all  $n \geq 1$ .

The rest of the article is organized as follows. Section 2 introduces our sparse tensor additive regression model. Section 3 develops an efficient penalized alternating minimization algorithm for model estimation. Section 4 investigates its theoretical properties, followed by simulation studies in Section 5 and a real online advertising application in Section 6. The appendix collects all technical proofs.

## 2 Sparse Tensor Additive Model

Given i.i.d. samples  $\{y_i, \mathcal{X}_i\}_{i=1}^n$ , our sparse tensor additive model assumes

$$y_i = \mathcal{T}^*(\mathcal{X}_i) + \epsilon_i = \sum_{j_1=1}^{p_1} \cdots \sum_{j_m=1}^{p_m} f_{j_1 \dots j_m}^*([\mathcal{X}_i]_{j_1 \dots j_m}) + \epsilon_i, \quad i = 1, \dots, n, \quad (2.1)$$

where  $f_{j_1 \dots j_m}^*(\cdot)$  is the nonparametric additive function belonging to some smooth function class  $\mathcal{H}$ , and  $\{\epsilon_i\}_{i=1}^n$  are i.i.d. observation noises.

Our STAR model utilizes spline series expansion (Huang et al., 2010; Fan et al., 2011) to approximate each individual nonparametric additive component. Let  $\mathcal{S}_n$  be the space of polynomial splines and  $\{\psi_h(x)\}_{h=1}^{d_n}$  be a normalized basis for  $\mathcal{S}_n$ , where  $d_n$  is the number of spline series and  $\sup_x |\psi_h(x)| \leq 1$ . It is known that for any  $f_n \in \mathcal{S}_n$ , there always exists some coefficients  $\{\beta_h^*\}_{h=1}^{d_n}$  such that  $f_n(x) = \sum_{h=1}^{d_n} \beta_h^* \psi_h(x)$ . In addition, under suitable smoothness assumptions (see Lemma 6.1), each nonparametric additive component  $f_{j_1 \dots j_m}^*(\cdot)$  can be well approximated by functions in  $\mathcal{S}_n$ . Applying the above approximation to each individual component, the regression function  $\mathcal{T}^*(\mathcal{X}_i)$  in (2.1) can be approximated by

$$\mathcal{T}^*(\mathcal{X}_i) \approx \sum_{j_1=1}^{p_1} \cdots \sum_{j_m=1}^{p_m} \sum_{h=1}^{d_n} \beta_{j_1 \dots j_m h}^* \psi_{j_1 \dots j_m h}([\mathcal{X}_i]_{j_1 \dots j_m}). \quad (2.2)$$

The expression in (2.2) has a compact tensor representation. Define  $\mathcal{F}_h(\mathcal{X}) \in \mathbb{R}^{p_1 \times \dots \times p_m}$  such that  $[\mathcal{F}_h(\mathcal{X})]_{j_1 \dots j_m} = \psi_{j_1 \dots j_m h}([\mathcal{X}]_{j_1 \dots j_m})$ , and  $\mathcal{B}_h^* \in \mathbb{R}^{p_1 \times \dots \times p_m}$  such that  $[\mathcal{B}_h^*]_{j_1 \dots j_m} = \beta_{j_1 \dots j_m h}^*$  for  $h \in [d_n]$ , where  $[k]$  denotes  $\{1, \dots, k\}$  for an integer  $k \geq 1$ . Consequently, we can write

$$\sum_{j_1=1}^{p_1} \cdots \sum_{j_m=1}^{p_m} \sum_{h=1}^{d_n} \beta_{j_1 \dots j_m h}^* \psi_{j_1 \dots j_m h}([\mathcal{X}_i]_{j_1 \dots j_m}) = \sum_{h=1}^{d_n} \langle \mathcal{B}_h^*, \mathcal{F}_h(\mathcal{X}_i) \rangle. \quad (2.3)$$

Therefore, the parameter estimation of the nonparametric additive model (2.1) reduces to the estimation of unknown tensor coefficients  $\mathcal{B}_1^*, \dots, \mathcal{B}_{d_n}^*$ . The coefficients  $\mathcal{B}_1^*, \dots, \mathcal{B}_{d_n}^*$  include a total

number of  $\mathcal{O}(d_n \prod_{j=1}^m p_j)$  free parameters, which could be much larger than the sample size  $n$ . In such ultrahigh-dimensional scenario, it is important to employ dimension reduction tools. A common tensor dimension reduction tool is the low-rank assumption (Chi and Kolda, 2012; Anandkumar et al., 2014; Yuan and Zhang, 2016; Sun et al., 2017). Similarly, we assume each coefficient tensor  $\mathcal{B}_1^*, \dots, \mathcal{B}_{d_n}^*$  satisfies the CP low-rank decomposition (Kolda and Bader, 2009):

$$\mathcal{B}_h^* = \sum_{r=1}^R \beta_{1hr}^* \circ \dots \circ \beta_{mhr}^*, \quad h = 1, \dots, d_n, \quad (2.4)$$

where  $\circ$  is the vector outer product,  $\beta_{1hr}^* \in \mathbb{R}^{p_1}, \dots, \beta_{mhr}^* \in \mathbb{R}^{p_m}$ , and  $R \ll \min\{p_1, \dots, p_m\}$  is the CP-rank. This formulation reduces the effective number of the parameters from  $\mathcal{O}(d_n \prod_{j=1}^m p_j)$  to  $\mathcal{O}(d_n \sum_{j=1}^m p_j)$ , and hence greatly improves computational efficiency. Under this formulation, our model can be written as

$$\mathcal{T}^*(\mathcal{X}_i) \approx \sum_{h=1}^{d_n} \left\langle \mathcal{F}_h(\mathcal{X}_i), \sum_{r=1}^R \beta_{1hr}^* \circ \dots \circ \beta_{mhr}^* \right\rangle. \quad (2.5)$$

**Remark 2.1.** Our model in (2.5) can be viewed as a generalization of several existing work. When  $\psi_{j_1 \dots j_m h}(\cdot)$  in (2.3) is an identity basis function ( $\psi_{j_1 \dots j_m h}([\mathcal{X}]_{j_1 \dots j_m}) = [\mathcal{X}]_{j_1 \dots j_m}$ ) with only one basis ( $d_n = 1$ ), (2.5) reduces to the bilinear form (Li et al., 2010; Hung and Wang, 2012) for a matrix covariate ( $m = 2$ ), and the multilinear form for linear tensor regression (Zhou et al., 2013; Hoff, 2015; Yu and Liu, 2016; Rabusseau and Kadri, 2016; Sun and Li, 2017; Guhaniyogi et al., 2017; Raskutti et al., 2019) for a tensor covariate ( $m \geq 3$ ).

In addition to the CP low-rank structure on the tensor coefficients, we further impose a group-type sparsity constraint on the components  $\beta_{khr}^*$ . This group sparsity structure not only further reduces the effective parameter size, but also improves the model interpretability, as it enables the variable selection of components in the tensor covariate. Recall that in (2.5) we have  $\beta_{khr}^* = (\beta_{khr1}^*, \dots, \beta_{khrp_k}^*)^\top$  for  $k \in [m], h \in [d_n], r \in [R]$ . We define our group sparsity constraint as

$$\underbrace{\left| \left\{ j \in [p_k] \mid \sum_{h=1}^{d_n} \sum_{r=1}^R \beta_{khrj}^{*2} \neq 0 \right\} \right|}_{\mathcal{S}_k} = s_k \ll p_k, \quad \text{for } k \in [m]. \quad (2.6)$$

where  $|\mathcal{S}_k|$  refers to the cardinality of the set  $\mathcal{S}_k$ . Figure 2 provides an illustration of the low-rank (2.4) and group-sparse (2.6) coefficients when the order of the tensor is  $m = 3$ . When  $m = 1$ , our model with the group sparsity constraint reduces to the vector sparse additive model (Ravikumar et al., 2009; Meier et al., 2009; Huang et al., 2010).

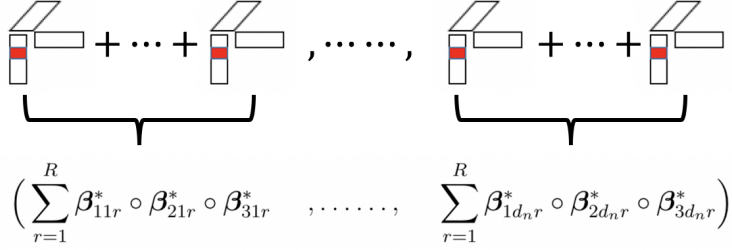


**Figure 2.** An illustration of the low-rank and group-sparse structures in a collection of three-way tensor coefficients  $(\mathcal{B}_1^*, \dots, \mathcal{B}_{d_n}^*)$ . If one or more of the coefficients at the colored locations are non-zero, the cardinality of  $\mathcal{S}_1$  increases by one.

### 3 Estimation

In this section, we describe our approach to estimate the parameters in our STAR model via a penalized empirical risk minimization which simultaneously satisfies the low-rankness and encourages the sparsity of decomposed components. In particular, we consider

$$\min_{\beta_{1hr}, \dots, \beta_{mhr}} \frac{1}{n} \sum_{i=1}^n \underbrace{\left( y_i - \sum_{h=1}^{d_n} \left\langle \sum_{r=1}^R \beta_{1hr} \circ \dots \circ \beta_{mhr}, \mathcal{F}_h(\mathcal{X}_i) \right\rangle \right)^2}_{\mathcal{L}(\beta_{1hr}, \dots, \beta_{mhr})} + \mathcal{P}(\beta_{1hr}, \dots, \beta_{mhr}), \quad (3.1)$$

where  $\mathcal{L}(\beta_{1hr}, \dots, \beta_{mhr})$  is the empirical risk function, in which the low-rankness is guaranteed due to the CP decomposition, and  $\mathcal{P}(\cdot)$  is a penalty term that encourages sparsity. To enforce the sparsity as defined in (2.6), we consider the group lasso penalty (Yuan and Lin, 2006), i.e.,

$$\mathcal{P}(\beta_{1hr}, \dots, \beta_{mhr}) = \sum_{k=1}^m \left( \lambda_{kn} \sum_{j=1}^{p_k} \sqrt{\sum_{h=1}^{d_n} \sum_{r=1}^R \beta_{khrj}^2} \right), \quad (3.2)$$

where  $\{\lambda_{kn}\}_{k=1}^m$  are tuning parameters. It is worth mentioning that our algorithm and theoretical analysis can accommodate a general class of decomposable penalties (see Condition 4.9 for details), which includes lasso, ridge, fused lasso, and group lasso as special cases.

For a general tensor covariate ( $m > 1$ ), the optimization problem in (3.1) is a non-convex optimization. This is fundamentally different from the vector sparse additive model (Ravikumar et al., 2009; Huang et al., 2010) whose optimization is convex. The non-convexity in (3.1) brings significant challenges in both model estimation and theoretical development. The key idea of our estimation procedure is to explore the bi-convex structure of the empirical risk function  $\mathcal{L}(\beta_{1hr}, \dots, \beta_{mhr})$  since it is convex in one argument while fixing all the other parameters. This



motivates us to rewrite the empirical risk function into a bi-convex representation, which in turn facilitates the introduction of an efficient alternating minimization algorithm.

Denote  $\vartheta_{krj} = (\beta_{k1rj}, \beta_{k2rj}, \dots, \beta_{kdnrj})^\top \in \mathbb{R}^{d_n \times 1}$ ,  $\vartheta_{kj} = (\vartheta_{k1j}^\top, \dots, \vartheta_{kRj}^\top)^\top \in \mathbb{R}^{Rd_n \times 1}$  for  $k \in [m]$ ,  $j \in [p_k]$ , and  $\mathbf{b}_k = (\vartheta_{k1}^\top, \dots, \vartheta_{kp_k}^\top)^\top$ . We also define the operator  $\prod_{k \in [m]}^\circ \mathbf{a}_k = \mathbf{a}_1 \circ \dots \circ \mathbf{a}_m$ . Remind that  $\mathcal{F}_h(\mathcal{X}) \in \mathbb{R}^{p_1 \times \dots \times p_m}$  with  $[\mathcal{F}_h(\mathcal{X})]_{j_1 \dots j_m} = \psi_{j_1 \dots j_m h}([\mathcal{X}]_{j_1 \dots j_m})$ , see (2.3). We use  $[\mathcal{F}_h^k(\mathcal{X}_i)]_j$  to refer to the  $m-1$  way tensor when we fix the index along the  $k$ -th way of  $\mathcal{F}_h(\mathcal{X}_i)$  as  $j$ , e.g.,  $[\mathcal{F}_h^1(\mathcal{X}_i)]_j \in \mathbb{R}^{p_2 \times \dots \times p_m}$ . Define

$$F_{irj}^k = \left( \left\langle \prod_{u \in [m] \setminus k}^\circ \beta_{u1r}, [\mathcal{F}_1^k(\mathcal{X}_i)]_j \right\rangle, \dots, \left\langle \prod_{u \in [m] \setminus k}^\circ \beta_{udnr}, [\mathcal{F}_{d_n}^k(\mathcal{X}_i)]_j \right\rangle \right)^\top, \quad (3.3)$$

and denote  $F_{ij}^k = (F_{i1j}^k, \dots, F_{iRj}^k)^\top \in \mathbb{R}^{Rd_n \times 1}$ . In addition, we denote  $\mathbf{F}_j^k = (F_{1j}^k, \dots, F_{nj}^k)^\top$ ,  $\mathbf{F}^k = (\mathbf{F}_1^k, \dots, \mathbf{F}_p^k)$ , and  $\mathbf{y} = (y_1, \dots, y_n)^\top$ . Thus, when other parameters are fixed, minimizing the empirical risk function (3.1) with respect to  $\mathbf{b}_k$  is equivalent to minimizing

$$\mathcal{L}(\mathbf{b}_1, \dots, \mathbf{b}_m) = \frac{1}{n} \|\mathbf{y} - \mathbf{F}^k \mathbf{b}_k\|_2^2. \quad (3.4)$$

Note that the expression of (3.4) holds for any  $k \in [m]$  with proper definitions on  $\mathbf{F}^k$  and  $\mathbf{b}_k$ .

Based on this reformulation, we are ready to introduce the alternating minimization algorithm that solves (3.1) by alternatively updating  $\mathbf{b}_1, \dots, \mathbf{b}_m$ . A desirable property of our algorithm is that updating  $\mathbf{b}_k$  given others can be solved efficiently via the back-fitting algorithm (Ravikumar et al., 2009). The detailed algorithm is summarized in Algorithm 1.

---

**Algorithm 1** Penalized Alternating Minimization for Solving (3.1)

---

- 1: **Input:**  $\{y_i\}_{i=1}^n$ ,  $\{\mathcal{X}_i\}_{i=1}^n$ , initialization  $\{\mathbf{b}_1^{(0)}, \dots, \mathbf{b}_m^{(0)}\}$ , the set of penalization parameters  $\{\lambda_{1n}, \dots, \lambda_{mn}\}$ , rank  $R$ , iteration  $t = 0$ , stopping error  $\epsilon = 10^{-5}$ .
- 2: Repeat  $t = t + 1$  and run penalized alternating minimization.
- 3: For  $k = 1$  to  $m$

$$\mathbf{b}_k^{(t+1)} = \underset{\mathbf{b}_k}{\operatorname{argmin}} \mathcal{L}(\mathbf{b}_1^{(t)}, \dots, \mathbf{b}_m^{(t)}) + \lambda_{kn} \mathcal{P}(\mathbf{b}_k^{(t)}), \quad (3.5)$$

where  $\mathcal{L}$  is defined in (3.4).

- 4: End for.
  - 5: Until  $\max_k \|\mathbf{b}_k^{(t+1)} - \mathbf{b}_k^{(t)}\|_2 \leq \epsilon$ , and let  $t = T^*$ .
  - 6: **Output:** the estimate of each component,  $\{\mathbf{b}_1^{(T^*)}, \dots, \mathbf{b}_m^{(T^*)}\}$ .
- 

In our implementation, we use ridge regression to initialize Algorithm 1, and set tuning parameters  $\lambda = \lambda_{kn}$  for  $k = 1, \dots, m$  for simplicity. The five-fold cross-validation is employed to select the best pair of the tuning parameter  $\lambda$  and the tensor rank  $R$  in our experiments.

## 4 Theory

In this section, we first establish a general theory for the penalized alternating minimization in the context of the tensor additive model. Several sufficient conditions are proposed to guarantee the optimization error and statistical error. Then, we apply our theory to the STAR estimator with B-spline basis functions and the group-lasso penalty. To ease the presentation, we consider a three-way tensor covariate (i.e,  $m = 3$ ) in our theoretical development, while its generalization to an  $m$ -way tensor is straightforward.

### 4.1 A general contract property

To bound the optimization error and statistical error of the proposed estimator, we introduce three sufficient conditions: a Lipschitz-gradient condition, a sparse strongly convex condition, and a generic statistical error condition. For the sake of brevity, we only present conditions for the update of  $\mathbf{b}_1$  in the main paper, and defer similar conditions for  $\mathbf{b}_2, \mathbf{b}_3$  to Section A2 in the appendix.

For each vector  $\mathbf{x} \in \mathbb{R}^{pd_n R \times 1}$ , we divide it into  $p$  equal-length segments as in Figure 3. A segment is colored if it contains at least one non-zero element, and a segment is uncolored if all of its elements are zero. We let  $w(\mathbf{x})$  be the number of colored segments in  $\mathbf{x}$  and  $E_s$  be the set of all  $(pd_n R)$ -dimensional vectors with less than  $C_0 s$  colored segments, for some constant  $C_0$ . Mathematically, for a vector  $\mathbf{x} \in \mathbb{R}^{pd_n R \times 1}$ , denote  $w(\mathbf{x}) := \{j \in [p] \mid \sum_{h=1}^{d_n R} x_{(j-1)d_n R+h}^2 \neq 0\}$  and  $E_s := \{\mathbf{x} \in \mathbb{R}^{pd_n R \times 1} \mid |w(\mathbf{x})| \leq C_0 s\}$ .

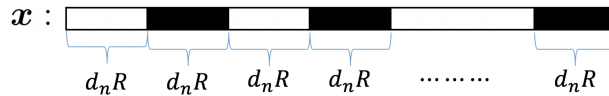


**Figure 3.** An illustration of the group sparse vector. A segment is colored if it contains at least one non-zero element, and a segment is uncolored if all of its elements are zero.

Define a sparse ball  $\mathcal{B}_{\alpha, s}(\mathbf{b}^*) := \{\mathbf{b} \in \mathbb{R}^{pd_n R} : \|\mathbf{b} - \mathbf{b}^*\|_2 \leq \alpha, \mathbf{b} \in E_s\}$  for a given constant radius  $\alpha$ . Moreover, the noisy gradient function and noiseless gradient function of empirical risk function  $\mathcal{L}$  defined in (3.1) of order-3 with respect to  $\mathbf{b}_1$  can be written as

$$\nabla_1 \mathcal{L}(\mathbf{b}_1, \mathbf{b}_2, \mathbf{b}_3) = \frac{2}{n} \mathbf{F}^{1\top} \left( \mathbf{F}^1 \mathbf{b}_1 - \mathbf{y} \right) \quad (4.1)$$

$$\nabla_1 \tilde{\mathcal{L}}(\mathbf{b}_1, \mathbf{b}_2, \mathbf{b}_3) = \frac{2}{n} \mathbf{F}^{1\top} \left( \mathbf{F}^1 \mathbf{b}_1 - \mathbf{F}^{1*} \mathbf{b}_1^* \right), \quad (4.2)$$

where  $F_{irj}^{1*} = (\langle \beta_{21r}^* \circ \beta_{31r}^*, [\mathcal{F}_1^1(\mathcal{X}_i)]_j \rangle, \dots, \langle \beta_{2d_n r}^* \circ \beta_{3d_n r}^*, [\mathcal{F}_{d_n}^1(\mathcal{X}_i)]_j \rangle)^\top$ .

**Condition 4.1** (Lipschitz-Gradient). For  $\mathbf{b}_2 \in \mathcal{B}_{\alpha_2, s_2}(\mathbf{b}_2^*)$ ,  $\mathbf{b}_3 \in \mathcal{B}_{\alpha_3, s_3}(\mathbf{b}_3^*)$ , the noiseless gradient function  $\nabla_1 \tilde{\mathcal{L}}(\mathbf{b}_1^*, \cdot, \mathbf{b}_3^*)$  satisfies  $\mu_{2n}$ -Lipschitz-gradient condition, and  $\nabla_1 \tilde{\mathcal{L}}(\mathbf{b}_1^*, \mathbf{b}_2, \cdot)$  satisfies  $\mu_{3n}$ -Lipschitz-gradient condition with high probability. That is,

$$\begin{aligned} \langle \nabla_1 \tilde{\mathcal{L}}(\mathbf{b}_1^*, \mathbf{b}_2, \mathbf{b}_3^*) - \nabla_1 \tilde{\mathcal{L}}(\mathbf{b}_1^*, \mathbf{b}_2^*, \mathbf{b}_3^*), \mathbf{b}_1 - \mathbf{b}_1^* \rangle &\leq \mu_{2n} \|\mathbf{b}_1 - \mathbf{b}_1^*\|_2 \|\mathbf{b}_2 - \mathbf{b}_2^*\|_2 \\ \langle \nabla_1 \tilde{\mathcal{L}}(\mathbf{b}_1^*, \mathbf{b}_2, \mathbf{b}_3) - \nabla_1 \tilde{\mathcal{L}}(\mathbf{b}_1^*, \mathbf{b}_2, \mathbf{b}_3^*), \mathbf{b}_1 - \mathbf{b}_1^* \rangle &\leq \mu_{3n} \|\mathbf{b}_1 - \mathbf{b}_1^*\|_2 \|\mathbf{b}_3 - \mathbf{b}_3^*\|_2, \end{aligned}$$

with probability at least  $1 - \delta_1$  for any  $0 < \delta_1 < 1$ . Here,  $\mu_{2n}, \mu_{3n}$  may depend on  $\delta_1$ .

**Remark 4.2.** Condition 4.1 defines a variant of Lipschitz continuity for  $\nabla_1 \tilde{\mathcal{L}}(\mathbf{b}_1^*, \cdot, \mathbf{b}_3^*)$  and  $\nabla_1 \tilde{\mathcal{L}}(\mathbf{b}_1^*, \mathbf{b}_2, \cdot)$ . Note that the gradient is always taken with respect to the first argument of  $\mathcal{L}(\cdot, \cdot, \cdot)$  and the Lipschitz continuity is with respect to the second or the third argument. Analogous Lipschitz-gradient conditions were also considered in Balakrishnan et al. (2017); Hao et al. (2017) for the *population-level Q-function* in the EM-type update.

Next condition characterizes the curvature of noisy gradient function in a sparse ball. It states that when the second and the third argument are fixed,  $\mathcal{L}(\cdot, \cdot, \cdot)$  is strongly convex with parameter  $\gamma_{1n}$  with high probability. As shown later in Section 4.2, this condition holds for a broad family of basis functions.

**Condition 4.3** (Sparse-Strong-Convexity). For any  $\mathbf{b}_2 \in \mathcal{B}_{\alpha_2, s_2}(\mathbf{b}_2^*)$ ,  $\mathbf{b}_3 \in \mathcal{B}_{\alpha_3, s_3}(\mathbf{b}_3^*)$ , the loss function  $\mathcal{L}(\cdot, \cdot, \cdot)$  is sparse strongly convex in its first argument, namely

$$\mathcal{L}(\mathbf{b}_1^*, \mathbf{b}_2, \mathbf{b}_3) - \mathcal{L}(\mathbf{b}_1, \mathbf{b}_2, \mathbf{b}_3) - \langle \nabla_1 \mathcal{L}(\mathbf{b}_1^*, \mathbf{b}_2, \mathbf{b}_3), \mathbf{b}_1^* - \mathbf{b}_1 \rangle \geq \frac{\gamma_{1n}}{2} \|\mathbf{b}_1 - \mathbf{b}_1^*\|_2^2,$$

with probability at least  $1 - \delta_2$  for any  $0 < \delta_2 < 1$ . Here,  $\gamma_{1n} > 0$  is the strongly convex parameter and may depend on  $\delta_2$ .

Next we present the definition for dual norm, which is a key measure for statistical error condition. More details on the dual norm are referred to Negahban et al. (2012).

**Definition 4.4** (Dual norm). For a given inner product  $\langle \cdot, \cdot \rangle$ , the dual norm of  $\mathcal{P}$  is given by

$$\mathcal{P}^*(\mathbf{v}) := \sup_{\mathbf{u} \in \mathbb{R}^p \setminus \{0\}} \frac{\langle \mathbf{u}, \mathbf{v} \rangle}{\mathcal{P}(\mathbf{u})}.$$

As a concrete example, the dual of  $\ell_1$ -norm is  $\ell_\infty$ -norm while the dual of  $\ell_2$ -norm is itself. Suppose  $\mathbf{v}$  is a  $p$ -dimensional vector and the index set  $\{1, 2, \dots, p\}$  is partitioned into  $N_{\mathcal{G}}$  disjoint groups, namely  $\mathcal{G} = \{G_1, \dots, G_{N_{\mathcal{G}}}\}$ . The group norm for  $\mathbf{v}$  is defined as  $\mathcal{P}(\mathbf{v}) = \sum_{t=1}^{N_{\mathcal{G}}} \|\mathbf{v}_{G_t}\|_2$ .

According to Definition (4.4), the dual of  $\mathcal{P}(\mathbf{v})$  is defined as  $\mathcal{P}^*(\mathbf{v}) = \max_t \|\mathbf{v}_{G_t}\|_2$ . For simplicity, we write  $\|\cdot\|_{\mathcal{P}^*} = \mathcal{P}^*(\cdot)$ .

The generic statistical error (SE) condition guarantees that the distance between noisy gradient and noiseless gradient under  $\mathcal{P}^*$ -norm is bounded.

**Condition 4.5** (Statistical-Error). For any  $\mathbf{b}_2 \in \mathcal{B}_{\alpha_2, s_2}(\mathbf{b}_2^*)$ ,  $\mathbf{b}_3 \in \mathcal{B}_{\alpha_3, s_3}(\mathbf{b}_3^*)$ , we have with probability at least  $1 - \delta_3$ ,

$$\|\nabla_1 \mathcal{L}(\mathbf{b}_1^*, \mathbf{b}_2, \mathbf{b}_3) - \nabla_1 \tilde{\mathcal{L}}(\mathbf{b}_1^*, \mathbf{b}_2, \mathbf{b}_3)\|_{\mathcal{P}^*} \leq \varepsilon_1.$$

**Remark 4.6.** Here,  $\varepsilon_1$  is only a generic quantity and its explicit form will be derived for a specific loss function in Section 4.2.

Next we introduce two conditions for the penalization parameter (Condition 4.7) and penalty (Condition 4.9). To illustrate Condition 4.7, we first introduce an quantity called *support space compatibility constant* to measure the intrinsic dimensionality of  $\mathcal{S}_1$  defined in (2.6) with respect to penalty  $\mathcal{P}$ . Specifically, it is defined as

$$\Phi(\mathcal{S}_1) := \sup_{\mathbf{b} \in \mathcal{S}_1 \setminus \{0\}} \frac{\mathcal{P}(\mathbf{b})}{\|\mathbf{b}\|_2}, \quad (4.3)$$

which is a variant of subspace compatibility constant originally proposed by Negahban et al. (2012) and Wainwright (2014). If  $\mathcal{P}(\mathbf{b})$  is chosen as a group lasso penalty, we have  $\Phi(\mathcal{S}') = \sqrt{|\mathcal{S}'|}$ , where  $\mathcal{S}'$  is the index set of active groups. Similar definitions of  $\Phi(\mathcal{S}_2), \Phi(\mathcal{S}_3)$  can be made accordingly.

**Condition 4.7** (Penalization Parameter). We consider an iterative turning procedure where tuning parameters in (3.5) are allowed to change with iteration. In particular, we assume tuning parameters  $\{\lambda_{1n}^{(t)}, \lambda_{2n}^{(t)}, \lambda_{3n}^{(t)}\}$  satisfy

$$\begin{aligned} \lambda_{1n}^{(t)} &= 4\varepsilon_1 + (\mu_{2n} \|\mathbf{b}_2^{(t)} - \mathbf{b}_2^*\|_2 + \mu_{3n} \|\mathbf{b}_3^{(t)} - \mathbf{b}_3^*\|_2) / \Phi(\mathcal{S}_1) \\ \lambda_{2n}^{(t)} &= 4\varepsilon_2 + (\mu'_{1n} \|\mathbf{b}_1^{(t)} - \mathbf{b}_1^*\|_2 + \mu'_{3n} \|\mathbf{b}_3^{(t)} - \mathbf{b}_3^*\|_2) / \Phi(\mathcal{S}_2) \\ \lambda_{3n}^{(t)} &= 4\varepsilon_3 + (\mu''_{1n} \|\mathbf{b}_1^{(t)} - \mathbf{b}_1^*\|_2 + \mu''_{2n} \|\mathbf{b}_2^{(t)} - \mathbf{b}_2^*\|_2) / \Phi(\mathcal{S}_3), \end{aligned} \quad (4.4)$$

where  $\{\mu_{2n}, \mu_{3n}\}, \{\mu'_{1n}, \mu'_{3n}\}, \{\mu''_{1n}, \mu''_{2n}\}$  are Lipschitz-gradient parameter which are defined in Condition 4.1 and Conditions 6.2-6.3.

**Remark 4.8.** Condition 4.7 considers an iterative sequence of regularization parameters. Given reasonable initializations for  $\mathbf{b}_1^{(t)}, \mathbf{b}_2^{(t)}, \mathbf{b}_3^{(t)}$ , their estimation errors gradually decay when the iteration  $t$  increases, which implies that  $\lambda_{kn}^{(t)}$  is a decreasing sequence. After sufficiently many iterations, the rate of the  $\lambda_{kn}^{(t)}$  will be bounded by the statistical error  $\varepsilon_k$ , for  $k = 1, 2, 3$ . This agrees with the

theory of high-dimensional regularized M-estimator in that suitable tuning parameter should be proportional to the target estimation error (Wainwright, 2014). Such iterative turning procedure plays a critical role in controlling statistical and optimization error, and has been commonly used in other high-dimensional non-convex optimization problems (Wang et al., 2014; Yi and Caramanis, 2015).

Finally, we present a general condition on the penalty term.

**Condition 4.9** (Decomposable Penalty). Given a space  $\mathcal{S}$ , a norm-based penalty  $\mathcal{P}$  is assumed to be decomposable with respect to  $\mathcal{S}$  such that it satisfies  $\mathcal{P}(\mathbf{u} + \mathbf{v}) = \mathcal{P}(\mathbf{u}) + \mathcal{P}(\mathbf{v})$  for any  $\mathbf{u} \in \mathcal{S}$  and  $\mathbf{v} \in \mathcal{S}^\perp$ , where  $\mathcal{S}^\perp$  is the complement of  $\mathcal{S}$ .

As shown in Negahban and Wainwright (2011), a broad class of penalties satisfies the decomposable property, such as lasso, ridge, fused lasso, group lasso penalties. Next theorem quantifies the error of one-step update for the estimator coming Algorithm 1.

**Theorem 4.10** (Contraction Property). Suppose Conditions 4.1,4.3,4.5,4.7, 6.2-6.7 hold. Assume the update at  $t$ -th iteration of Algorithm 1,  $\mathbf{b}_1^{(t)}, \mathbf{b}_2^{(t)}, \mathbf{b}_3^{(t)}$  fall into sparse balls  $\mathcal{B}_{\alpha_1, s_1}(\mathbf{b}_1^*), \mathcal{B}_{\alpha_2, s_2}(\mathbf{b}_2^*), \mathcal{B}_{\alpha_3, s_3}(\mathbf{b}_3^*)$  respectively, where  $\alpha_1, \alpha_2, \alpha_3$  are some constants. Define  $\mathcal{E}^{(t)} = \|\mathbf{b}_1^{(t)} - \mathbf{b}_1^*\|_2^2 + \|\mathbf{b}_2^{(t)} - \mathbf{b}_2^*\|_2^2 + \|\mathbf{b}_3^{(t)} - \mathbf{b}_3^*\|_2^2$ . There exists absolute constant  $C_0 > 1$  such that, the estimation error of the update at the  $t + 1$ -th iteration satisfies,

$$\mathcal{E}^{(t+1)} \leq \rho \mathcal{E}^{(t)} + C_0 \left( \frac{\varepsilon_1^2 \Phi(\mathcal{S}_1)^2}{\gamma_{1n}^2} + \frac{\varepsilon_2^2 \Phi(\mathcal{S}_2)^2}{\gamma_{2n}^2} + \frac{\varepsilon_3^2 \Phi(\mathcal{S}_3)^2}{\gamma_{3n}^2} \right), \quad (4.5)$$

with probability at least  $1 - 3(\delta_1 + \delta_2 + \delta_3)$ . Here,  $\rho$  is the contraction parameter defined as

$$\rho = C_1 \max\{\mu_{1n}'^2, \mu_{1n}''^2, \mu_{2n}'^2, \mu_{2n}''^2, \mu_{3n}'^2, \mu_{3n}''^2\} / \min\{\gamma_{1n}^2, \gamma_{2n}^2, \gamma_{3n}^2\}, \quad (4.6)$$

where  $C_1$  is some constant.

Theorem 4.10 demonstrates the mechanism of how the estimation error improves in the one-step update. When the the contraction parameter  $\rho$  is strictly less than 1 (we will prove that it holds for certain class of basis functions and penalties in next section), the first term of RHS in (4.5) will gradually go towards zero and the second term will be stable. The contraction parameter  $\rho$  is roughly the ratio of Lipschitz-gradient parameter and the strongly convex parameter. Similar formulas of contraction parameter frequently appears in the literature of statistical guarantees for low/high-dimensional non-convex optimization (Balakrishnan et al., 2017; Yi and Caramanis, 2015; Hao et al., 2017).

## 4.2 Application to STAR estimator

In this section, we apply the general contract property in Theorem 4.10 to STAR estimator with B-spline basis functions. The formal definition of B-spline basis function is defined in Section A1 of the appendix. To ensure Conditions 4.1-4.3 and 4.5 are satisfied, in our STAR estimator we require conditions on the nonparametric component, the distribution of tensor covariate and the noise distribution.

**Condition 4.11** (Function Class). Each nonparametric component in (1.1) is assumed to belong to the function class  $\mathcal{H}$  defined as follows,

$$\mathcal{H} = \left\{ g(\cdot) : |g^{(r)}(s) - g^{(r)}(t)| \leq C|s - t|^\alpha, \text{ for } s, t \in [a, b] \right\}. \quad (4.7)$$

Let  $\kappa = r + \alpha > 0.5$  be the smoothness parameter of function class  $\mathcal{H}$ . For  $j \in [p_1], k \in [p_2], l \in [p_3]$ , there is a constant  $c_f > 0$  such that  $\min_{jkl} \|f_{jkl}^*(x)\|_2 \geq c_f$  and  $\mathbb{E}(f_{jkl}^*([\mathcal{X}]_{jkl})) = 0$ . Each component of the covariate tensor  $\mathcal{X}$  has an absolutely continuous distribution and its density function is bounded away from zero and infinitely on  $C$ .

Condition 4.11 is classical for nonparametric additive model (Stone, 1985; Huang et al., 2010; Fan et al., 2011). Such condition is required to optimally estimate each individual additive component in  $\ell_2$ -norm.

**Condition 4.12** (Sub-Gaussian Noise). The noise  $\{\epsilon_i\}_{i=1}^n$  are i.i.d. randomly generated with mean 0 and bounded variance  $\sigma^2$ . Moreover,  $(\epsilon_i/\sigma)$  is sub-Gaussian distributed, i.e., there exists constant  $C_\epsilon > 0$  such that  $\|(\epsilon_i/\sigma)\|_{\phi_2} := \sup_{p \geq 1} p^{-1/2} (\mathbb{E}|\epsilon_i/\sigma|^p)^{1/p} \leq C_\epsilon$ , and independent of tensor covariates  $\{\mathcal{X}_i\}_{i=1}^n$ .

**Condition 4.13** (Parameter Space). We assume the absolute value of maximum entry of  $(\mathbf{b}_1^{*\top}, \mathbf{b}_2^{*\top}, \mathbf{b}_2^{*\top})$  is upper bounded by some positive constant  $c^*$ , and the absolute value of minimum non-zero entry of  $(\mathbf{b}_1^{*\top}, \mathbf{b}_2^{*\top}, \mathbf{b}_2^{*\top})$  is lower bounded by some positive constant  $c_*$ . Here,  $c^*, c_*$  not depending on  $n, p$ . Moreover, we assume the CP-rank  $R$  and sparsity parameters  $s_1, s_2, s_3$  are bounded by some constants.

**Remark 4.14.** The condition of bounded elements of tensor coefficient widely appears in tensor literature (Anandkumar et al., 2014; Sun et al., 2017). Here the bounded tensor rank condition is imposed purely for simplifying the proofs and this condition is possible to relax to allow slowly increased tensor rank (Sun and Li, 2018). The fixed sparsity assumption is also required in the vector nonparametric additive regression (Huang et al., 2010). To relax it, Meier et al. (2009)

considered a diverging sparsity scenario but required a compatibility condition which was hard to verify in practice. Thus, in this paper we consider a fixed sparsity case and leave the extension of diverging sparsity as future work.

Since the penalized empirical risk minimization (3.1) is a highly non-convex optimization, we require some conditions on the initial update in Algorithm 1.

**Condition 4.15** (Initialization). The initialization of  $\mathbf{b}_1, \mathbf{b}_2, \mathbf{b}_3$  is assumed to fall into a sparse constant ball centered at  $\mathbf{b}_1^*, \mathbf{b}_2^*, \mathbf{b}_3^*$ , saying  $\mathbf{b}_1^{(0)} \in \mathcal{B}_{\alpha_1, s_1}(\mathbf{b}_1^*), \mathbf{b}_2^{(0)} \in \mathcal{B}_{\alpha_2, s_1}(\mathbf{b}_2^*), \mathbf{b}_3^{(0)} \in \mathcal{B}_{\alpha_3, s_1}(\mathbf{b}_3^*)$ , where  $\alpha_1, \alpha_2, \alpha_3$  are some constants that are not diverging with  $n, p$ .

**Remark 4.16.** Similar initialization conditions have been widely used in tensor decomposition (Sun et al., 2017; Sun and Li, 2018), tensor regression (Suzuki et al., 2016; Sun and Li, 2017), and other non-convex optimization (Wang et al., 2014; Yi and Caramanis, 2015). Another line of work considers to design spectral methods to initialize certain simple non-convex optimization, such as matrix completion (Ma et al., 2017) and tensor sketching (Hao et al., 2018). The success of spectral methods heavily relies on a simple non-convex geometry and explicit form of high-order moment calculation, which is easy to achieve in previous work (Ma et al., 2017; Hao et al., 2018) by assuming a Gaussian error assumption. However, the design of spectral method in our tensor additive regression is substantially harder since the high-order moment calculation has no explicit form in our context. We leave the design of spectral-based initialization as future work.

Finally, we state the main theory on the estimation error of our STAR estimator with B-spline basis functions and a group lasso penalty.

**Theorem 4.17.** Suppose Conditions 4.7, 4.11-4.13, 4.15 hold and consider the class of normalized B-spline basis functions defined in (A1) and group-lasso penalty defined in (3.2). If one chooses the number of spline series  $d_n \asymp n^{\frac{1}{2\kappa+1}}$ , with probability at least  $1 - C_0(t+1)(sn^{-\frac{2\kappa}{2\kappa+1}} + 1/p)$ , we have

$$\mathcal{E}^{(t+1)} \leq \underbrace{\rho^{t+1} \mathcal{E}^{(0)}}_{\text{optimization error}} + \underbrace{\frac{C_1}{1-\rho} n^{-\frac{2\kappa-1}{2\kappa+1}} \log(pd_n)}_{\text{statistical error}}, \quad (4.8)$$

where  $0 < \rho \leq 1/2$  is a contraction parameter, and  $\kappa$  is the smoothness parameter of function class  $\mathcal{H}$  in (4.7). Consequently, when the total number of iterations is no smaller than

$$T^* = \log \left( \frac{1-\rho}{C_1 \mathcal{E}^{(0)}} \frac{n^{\frac{2\kappa-1}{2\kappa+1}}}{\log(pd_n)} \right) / \log(1/\rho),$$

and the sample size  $n \geq C_2(\log p)^{\frac{2\kappa+1}{2\kappa-1}}$  for sufficiently large  $C_2$ , we have

$$\mathcal{E}^{(T^*)} \leq \frac{2C_1}{1-\rho} n^{-\frac{2\kappa-1}{2\kappa+1}} \log(pd_n),$$

with probability at least  $1 - C_0(T^* + 1)(sn^{-\frac{2\kappa}{2\kappa+1}} + 1/p)$ .

The non-asymptotic estimation error bound (4.8) consists of two parts: an optimization error which is incurred by the non-convexity and a statistical error which is incurred by the observation noise and the spline approximation. Here, optimization error decays geometrically with the iteration number  $t$ , while the statistical error remains the same when  $t$  grows. When the tensor covariate is of order-one, i.e., a vector covariate, the overall optimization problem reduces to classical vector nonparametric additive model. In that case, we do not have the optimization error ( $\rho^{t+1}\mathcal{E}^{(0)}$ ) any more since the whole optimization is convex, and the statistical error term matches the state-of-the-art rate in Huang et al. (2010).

Lastly, let us define  $\widehat{\mathcal{T}}(\mathcal{X}) = \sum_{h=1}^{d_n} \sum_{r=1}^R \langle \beta_{1hr}^{(T^*)} \circ \beta_{2hr}^{(T^*)} \circ \beta_{3hr}^{(T^*)}, \mathcal{F}_h(\mathcal{X}) \rangle$  as a final estimator of the target function  $\mathcal{T}^*(\mathcal{X})$ . The following corollary provides the final error rate for the estimation of tensor additive nonparametric function  $\mathcal{T}^*(\mathcal{X})$ . It incorporates the approximation error of nonparametric component incurred by the B-spline series expansion, and the estimation error of unknown tensor parameter incurred by noises.

**Corollary 4.18.** Suppose Conditions 4.7, 4.11-4.13, 4.15 hold and the number of iterations  $t$  as well as the sample size  $n$  satisfy the requirement in Theorem 4.17. Then, the final estimator satisfies

$$\|\widehat{\mathcal{T}}(\mathcal{X}) - \mathcal{T}^*(\mathcal{X})\|_2^2 = \mathcal{O}_p\left(n^{-\frac{2\kappa}{2\kappa+1}} \log(pd_n)\right).$$

## 5 Simulations

In this section, we carry out intensive simulation studies to evaluate the performance of our STAR method, and compare it with existing competing solutions including the tensor linear regression (TLR) (Zhou et al., 2013), the Gaussian process based nonparametric method (GP) (Kanagawa et al., 2016), and the nonlinear tensor regression via alternative minimization procedure (AMP) (Suzuki et al., 2016). We find that STAR enjoys better performance both in terms of prediction accuracy and computational efficiency.

### 5.1 Low-rank covariate structure

The simulated data are generated based on the following model,

$$y_i = \mathcal{T}^*(\mathcal{X}_i) + \sigma\epsilon_i, \quad i = 1, \dots, n, \quad (5.1)$$

where  $\epsilon_i \sim N(0, 1)$ . For each observation,  $y_i \in \mathbb{R}$  is the response and  $\mathcal{X}_i \in \mathbb{R}^{p_1 \times p_2}$  is the two-way tensor (matrix) covariate. We fix  $p_2 = 8$ , and we vary  $n$  from  $\{400, 600\}$ ,  $p_1$  from  $\{20, 50, 100\}$ , and



$\sigma$  from  $\{0.1, 1\}$ . We assume that there are 10 and 4 important features along the first and second way of  $\mathcal{X}$ , respectively.

Since both GP and AMP models require a low-rank structure on the tensor covariates, in this simulation we consider the low-rank covariate case which favors their models. For each  $i = 1, \dots, n$ , we consider  $\mathcal{X}_i = \mathbf{x}_i^{(1)} \circ \mathbf{x}_i^{(2)}$ , where the elements of  $\mathbf{x}_i^{(1)} \in \mathbb{R}^{p_1}$  and  $\mathbf{x}_i^{(2)} \in \mathbb{R}^{p_2}$  are independently and identically distributed from uniform distribution. Following the additive model that is considered in [Ravikumar et al. \(2009\)](#), we generate samples according to

$$y_i = \sum_{j=1}^4 \sum_{k=1}^4 \mathcal{T}_j^*([\mathbf{x}_i^{(1)}]_j) \cdot \mathcal{T}_k^*([\mathbf{x}_i^{(2)}]_k) + \sigma \epsilon_i, \quad i = 1, \dots, n,$$

where the nonlinear functions  $\mathcal{T}_j^*$  and  $\mathcal{T}_k^*$  are given by

$$\mathcal{T}_j^*(x) = \begin{cases} -\sin(1.5x), & \text{if } j \text{ is odd,} \\ x^3 + 1.5(x - 0.5)^2, & \text{if } j \text{ is even,} \end{cases} \quad \text{and} \quad \mathcal{T}_k^*(x) = \begin{cases} -\phi(x, 0.5, 0.8^2), & \text{if } k \text{ is odd,} \\ \sin\{\exp(-0.5x)\}, & \text{if } k \text{ is even.} \end{cases}$$

Here  $\phi(\cdot, 0.5, 0.8^2)$  is the probability density function of the normal distribution  $N(0.5, 0.8^2)$ .

[Table 1](#) compares the mean squared error (MSE) of all four models, where MSE is assessed on an independently generated test data of 2,000 samples. The STAR model shows the lowest MSE in all cases. As expected, the TLR model has unsatisfactory performance, as the true regression model is non-linear. The two nonparametric tensor regression models GP and AMP can capture partial nonlinear structures, however, our method still outperform theirs.

Next, we investigate the computational costs of all four methods. [Table 2](#) compares the computation time in the example with  $n = 400$  and  $\sigma = 0.1$ . The results of other scenarios are similar and hence omitted. All the computation time includes the model fitting and the model tuning using five-fold cross-validation. Overall our STAR method is as fast as AMP and is much faster than GP. When the tensor dimension is small,  $p_1 = 20$ , the linear model TLR is the fastest one, however, its computation cost dramatically increase when the dimension  $p_1$  increases, and is even slower than other nonparametric models when  $p_1 = 100$ . On the other hand, the computation time of our model is less sensitive to the dimensionality and is even faster than TLR when  $p_1$  is large. This indicates the importance of fully exploiting the low-rankness and sparsity structures in order to improve computational efficiency.

## 5.2 General covariate structure

The settings are similar as that in [Section 5.1](#), except that the covariate is not low-rank. Here, the elements of  $\mathcal{X}_i \in \mathbb{R}^{p_1 \times p_2}$  are independently and identically distributed from uniform distribution. In

**Table 1.** *MSE of simulated data with low-rank covariate structure.*

$(n, \sigma)$	model	$p_1 = 20$		$p_1 = 50$		$p_1 = 100$	
(400, 0.1)	<b>STAR</b>	0.51	(0.01)	0.53	(0.01)	0.50	(0.01)
	TLR	2.03	(0.17)	2.63	(0.17)	3.16	(0.48)
	AMP	1.02	(0.02)	1.01	(0.02)	1.01	(0.02)
	GP	1.02	(0.01)	1.03	(0.03)	1.02	(0.01)
(600, 0.1)	<b>STAR</b>	0.50	(0.01)	0.50	(0.01)	0.52	(0.01)
	TLR	2.11	(0.09)	2.81	(0.14)	3.19	(0.21)
	AMP	0.99	(0.02)	1.01	(0.00)	1.00	(0.02)
	GP	0.99	(0.02)	1.01	(0.01)	1.02	(0.01)
(400, 1)	<b>STAR</b>	1.54	(0.02)	1.59	(0.03)	1.56	(0.01)
	TLR	2.29	(0.17)	3.18	(0.40)	4.91	(0.56)
	AMP	1.98	(0.02)	2.01	(0.01)	2.06	(0.03)
	GP	2.05	(0.04)	2.04	(0.03)	2.07	(0.03)
(600, 1)	<b>STAR</b>	1.55	(0.01)	1.53	(0.01)	1.54	(0.01)
	TLR	2.89	(0.39)	3.90	(0.36)	4.69	(0.46)
	AMP	2.02	(0.02)	2.03	(0.03)	2.04	(0.03)
	GP	2.02	(0.01)	2.04	(0.04)	2.06	(0.03)

\* The simulation compares sparse tensor additive regression (STAR), tensor linear regression (TLR), alternative minimizing procedure (AMP), and Gaussian process (GP). The reported errors are the medians over 20 independent runs, and the standard error of the medians are given in parentheses. All the methods use five-fold cross-validation procedures to tune the parameters.

particular, we generate  $n$  observations according to

$$y_i = \sum_{j=1}^4 \sum_{k=1}^4 \mathcal{T}_{jk}^*([\mathcal{X}_i]_{jk}) + \sigma \epsilon_i, \quad i = 1, \dots, n,$$

where

$$\mathcal{T}_{jk}^*(x) = \begin{cases} -\sin(1.5x), & \text{if } j \text{ is odd and } k \text{ is odd,} \\ x^3 + 1.5(x - 0.5)^2, & \text{if } j \text{ is even and } k \text{ is odd,} \\ -\phi(x, 0.5, 0.8^2), & \text{if } j \text{ is odd and } k \text{ is even,} \\ \sin\{\exp(-0.5x)\}, & \text{if } j \text{ is even and } k \text{ is even.} \end{cases} \quad (5.2)$$

**Table 2.** The computation time of all methods in Section 5.1 with  $n = 400$  and  $\sigma = 0.1$ .

$p_1$	20	50	100
<b>STAR</b>	353.30	227.65	391.90
TLR	156.19	738.96	1803.49
AMP	330.74	336.10	341.15
GP	1841.51	1913.27	1792.50

\* All the time include five-fold cross-validation procedures to tune the parameters. The results are averaged over 20 independent runs. The experiment was conducted using a single processor Inter(R) Xeon(R) CPU E5-2600@2.60GHz.

The comparisons of the MSE are summarized in Table 3: the MSE of the STAR model is much lower than that of all the other three models. Similar to the experiment in Section 5.1, the large MSE of TLR is attributed to the incapability of capturing the nonlinear relationship in the additive model. In this example, the GP and AMP models deliver relatively large MSE because the assumption of low-rank covariate structure is violated. Importantly, the MSE of our STAR model decreases, as the sample size increases, or the dimensionality  $p_1$  increases, or the noise level  $\sigma$  decreases. These observations align with our theoretical finding in Theorem 4.17.

### 5.3 Three-way covariate structure

We next extend the previous simulations to a three-way covariate structure. We consider two cases in this section. In the first case, we generate the tensor covariate  $\mathcal{X}_i \in \mathbb{R}^{p_1 \times p_2 \times 2}$  whose elements are from i.i.d. uniform distribution, and then generate the response  $y_i \in \mathbb{R}$  from

$$\text{case 1: } y_i = \sum_{j=1}^4 \sum_{k=1}^4 [\sin(\mathcal{T}_{jk1}^*([\mathcal{X}_i]_{jk1})) + \log |\mathcal{T}_{jk2}^*([\mathcal{X}_i]_{jk2})|] + \sigma \epsilon_i, \quad i = 1, \dots, n,$$

where  $\mathcal{T}_{jkl}^*$  with  $l = 1, 2$  is defined the same as the expression (5.2). In the second case, we generate the response from

$$\text{case 2: } y_i = \sin \left( \sum_{j=1}^4 \sum_{k=1}^4 \mathcal{T}_{jk}^*([\mathcal{X}_i]_{jkl}) \right) + \log \left| \sum_{j=1}^4 \sum_{k=1}^4 \mathcal{T}_{jk}^*([\mathcal{X}_i]_{jkl}) \right| + \sigma \epsilon_i, \quad i = 1, \dots, n.$$

**Table 3.** *MSE of simulated data with general covariate structure.*

$(n, \sigma)$	model	$p_1 = 20$		$p_1 = 50$		$p_1 = 100$	
(400, 0.1)	<b>STAR</b>	2.30	(0.06)	3.34	(0.22)	5.04	(0.33)
	TLR	40.62	(0.53)	53.94	(0.71)	92.31	(1.60)
	AMP	41.09	(0.31)	40.78	(0.35)	40.97	(0.30)
	GP	41.62	(0.24)	41.35	(0.38)	41.18	(0.22)
(600, 0.1)	<b>STAR</b>	1.76	(0.04)	2.14	(0.11)	2.53	(0.12)
	TLR	37.12	(0.63)	43.74	(0.85)	58.75	(0.88)
	AMP	40.39	(0.30)	40.35	(0.35)	41.00	(0.37)
	GP	40.65	(0.66)	40.57	(0.64)	41.28	(0.44)
(400, 1)	<b>STAR</b>	3.98	(0.11)	5.28	(0.26)	7.17	(0.50)
	TLR	42.12	(0.51)	56.47	(0.78)	94.09	(2.38)
	AMP	42.00	(0.38)	42.40	(0.47)	41.51	(0.28)
	GP	42.56	(0.36)	42.19	(0.37)	42.08	(0.30)
(600, 1)	<b>STAR</b>	3.13	(0.05)	3.63	(0.13)	4.10	(0.11)
	TLR	38.06	(0.59)	45.43	(0.65)	60.20	(1.03)
	AMP	41.44	(0.54)	41.99	(0.45)	41.76	(0.40)
	GP	41.31	(0.50)	41.87	(0.44)	42.49	(0.53)

\* The simulation compares sparse tensor additive regression (STAR), tensor linear regression (TLR), alternative minimizing procedure (AMP), and Gaussian process (GP). The reported errors are the medians over 20 independent runs, and the standard error of the medians are given in parentheses. All the methods use five-fold cross-validation procedures to tune the parameters.

It is worth noting that case 1 uses an additive model while case 2 does not. Therefore, the additive model assumption in our STAR method is actually mis-specified in case 2.

Since the AMP and GP models are only applicable for two-way tensor covariates, in this simulation we only compare our STAR model with TLR. We vary the sample size  $n \in \{600, 1000\}$ , the first-way dimension  $p_1 \in \{20, 50, 200\}$ , the noise level  $\sigma \in \{0.1, 1\}$ , and fix the second-way dimension  $p_2 = 10$ . Similar to previous simulations, we assume that there are 10, 4, and 2 important features along the three modes of the tensor  $\mathcal{X}_i$ , respectively. As shown in Table 4, the MSE of the STAR model is consistently lower than that of TLR, even in the case when the additive model is mis-specified.

**Table 4.** *MSE of simulated data with three-way tensor covariates.*

		$p_1 = 20$		$p_1 = 50$		$p_1 = 200$	
<b>Case 1</b>							
(600, 0.1)	<b>STAR</b>	0.34	(0.03)	1.33	(0.23)	1.10	(0.03)
	TLR	10.69	(0.06)	10.86	(0.14)	13.47	(0.25)
(600, 1)	<b>STAR</b>	1.45	(0.02)	1.71	(0.20)	1.99	(0.01)
	TLR	11.93	(0.09)	12.45	(0.14)	18.14	(0.95)
(1000, 0.1)	<b>STAR</b>	0.37	(0.02)	0.43	(0.03)	1.24	(0.25)
	TLR	10.82	(0.10)	10.77	(0.12)	11.68	(0.11)
(1000, 1)	<b>STAR</b>	1.40	(0.03)	1.47	(0.02)	2.02	(0.03)
	TLR	11.90	(0.06)	11.98	(0.15)	13.58	(0.19)
<b>Case 2</b>							
(600, 0.1)	<b>STAR</b>	0.78	(0.01)	2.07	(1.10)	1.01	(0.00)
	TLR	13.11	(0.11)	13.11	(0.17)	16.62	(0.33)
(600, 1)	<b>STAR</b>	2.07	(0.08)	2.01	(0.02)	1.99	(0.02)
	TLR	14.45	(0.17)	14.33	(0.14)	20.73	(0.66)
(1000, 0.1)	<b>STAR</b>	0.75	(0.00)	0.78	(0.05)	1.35	(0.17)
	TLR	13.15	(0.22)	12.98	(0.17)	13.52	(0.23)
(1000, 1)	<b>STAR</b>	1.76	(0.02)	2.13	(0.12)	1.99	(0.02)
	TLR	14.15	(0.29)	14.05	(0.19)	15.57	(0.27)

\* The simulation compares sparse tensor additive regression (STAR) and tensor linear regression (TLR). The reported errors are the medians over 20 independent runs, and the standard error of the medians are given in parentheses. All the methods use five-fold cross-validation procedures to tune the parameters.

## 6 An Application to Online Advertising

In this section, we apply the STAR model to click-through rate (CTR) prediction in online advertising. The CTR is defined to be the ratio between the number of clicks and the number of impressions (ad views). In this study, we are interested in predicting the overall CTR, which is the average CTR across different ad campaigns. The overall CTR is an effective measure to evaluate the performance of online advertising. A low overall CTR usually indicates that the ads are not effectively displayed or the wrong audience is being targeted. As a reference, the across-industry overall CTR of display campaigns in the United States from April 2016 to April 2017 is 0.08%.<sup>1</sup> Importantly, the CTR is also closely related to the revenue. Define the effective revenue per mile (eRPM) to be the amount

<sup>1</sup>The data are from <http://www.richmediagallery.com/learn/benchmarks>.

of revenue from every 1000 impressions, and we have  $eRPM = 1000 \times CPC \times CTR$ , where CPC is the cost per click. From this expression, we can see that a good CTR prediction is critical to ad pricing, and the CTR prediction is a highly important task in online advertising.

We collect 125 ad campaign data during 28 days from a premium Internet media company.<sup>2</sup> The data from each day have been aggregated into six time periods and each of the 125 campaigns involves ads delivered via three devices: phone, tablet, and personal computer (PC). In total, we have  $168 = 28 \times 6$  time periods. For each time period, we aggregate the number of impressions of 125 advertising campaigns that are delivered on each of three types of devices among 153 million of users. We denote the number of impressions across 125 ad campaigns and 3 devices by a matrix  $\mathcal{X}_i \in \mathbb{R}^{125 \times 3}$ , and the overall CTR as  $y_i$ , for each time period  $i = 1, 2, \dots, 168$ . In this study, we aim to study the relationship between the overall CTR and the two-way tensor covariate of impressions.

Figure 1 delineates the marginal relationship between the overall CTR and the impression of one advertisement that is delivered on phone, tablet, and PC, respectively. In this example, the overall CTR clearly reveals a non-linear pattern across all devices. Moreover, it is generally believed that not all ads have significant impacts on the overall CTR and hence ad selection is an active research area (Choi et al., 2010; Xu et al., 2016). To fulfill both tasks of capturing the nonlinear relationship and selecting important ads, we apply the proposed STAR model to predict the overall CTR. The logarithm transformations are applied to both the CTR and the number of impressions. We train and tune each method on the data obtained on the first 20 days, and use the remaining data as the test data to assess the prediction accuracy. Table 5 compares the MSE and run time of our STAR model with those of TLR, GP, and AMP models. It is seen that our STAR method delivers the best performance both in terms of the prediction accuracy and the computational time. This result shows the effectiveness of the low-rankness and group sparsity structures both in increasing the CTR prediction accuracy and the algorithm efficiency.

---

<sup>2</sup>The reported data and results in this section are deliberately incomplete and subject to anonymization, and thus do not necessarily reflect the real portfolio at any particular time.

**Table 5.** CTR prediction error and computational time (in seconds).

method	MSE	time
<b>STAR</b>	0.053	5.843
TLR	0.174	96.029
AMP	0.100	62.026
GP	0.127	6389.441

In terms of ad selection, the STAR model with group lasso penalty selects 34 out of 125 ads, and selects all three devices as active variables for the CTR prediction. Among the 34 ads selected by our model, 10 are related to the shopping category and 7 belongs to the travel category. As a comparison, TLR selects 79 ads, 27 of which are also selected by our STAR method. The GP and AMP models cannot perform variable selection. Besides the prediction on the overall CTR and the ad selection performance, we are also able to see which ad and device combination yields the most significant impact on the overall CTR. In the left panel of Figure 4, each tile represents a combination of ad and device, and the darkness of the tile implies the sensitivity of the overall CTR associated with one more impression on this combination. In general, we observe that the overall CTR is most sensitive to ads delivered on the phone device. Displayed on phones, the ad with ID 5 has the largest positive impact on the overall CTR, and the ad with ID 101 has the most negative effect. The right panel of Figure 4 is constructed similarly except for that the change is due to every 1000 additional impressions on the certain combinations, in which case the overall CTR has the largest growth when 1000 impressions are allocated to the ad with ID 84 displaying on phones. This indicates the nonlinear relationship between the overall CTR and the number of impressions. This result is important for managerial decision making. Under a specific budget for additional ad allocations, our STAR model is feasible to provide the best ad/device combination to increase the ad revenue.

## Appendix

In the appendix, we present the definition and properties of the B-spline basis, and some additional conditions for our theoretical results. The proofs of all the lemmas and theorems are deferred to supplementary materials, which is available upon request.

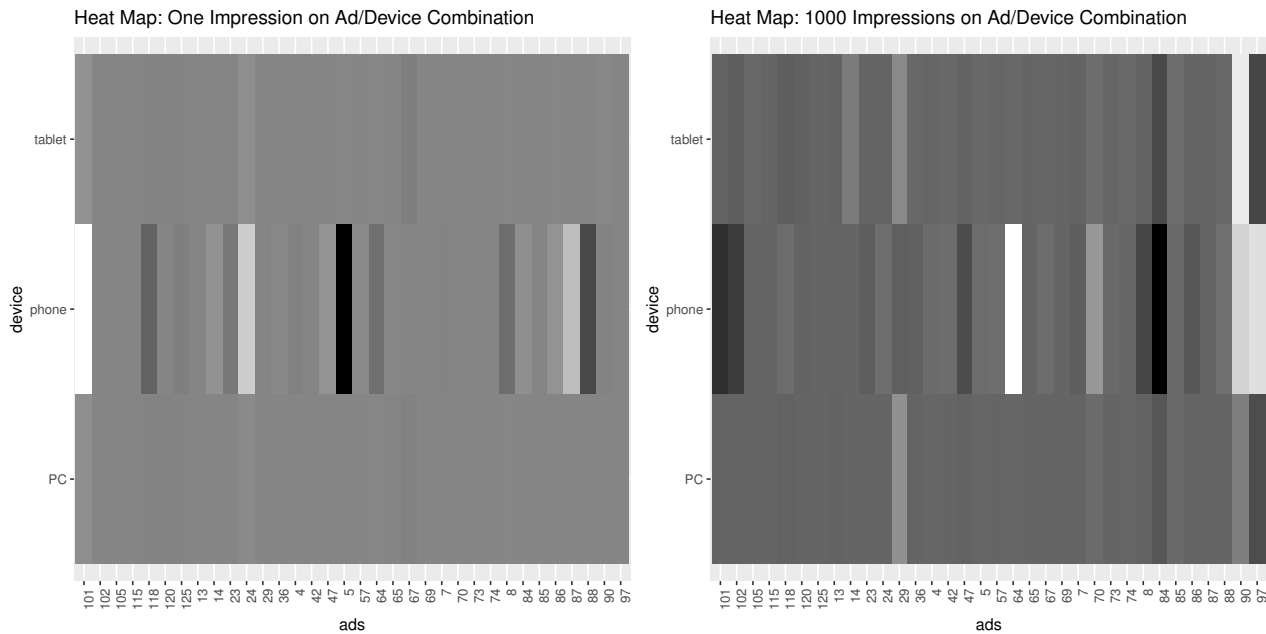


**Figure 4.** Heatmaps for the overall CTR. The left panel shows the mean change in the overall CTR if the test data have one additional impression on each ad and device combination. The right panel shows the average increase for each additional 1000 impressions on certain ad and device combinations. Darker tiles indicate greater positive mean change in the overall CTR and lighter tiles indicate greater negative mean change. The ad IDs have been renumbered for concerns of confidentiality.

## A1 Properties of B-spline

We formally define the  $q$ -th order B-splines with a set of  $m$  internal knot sequences  $k = \{0 = k_0 < k_1 < \dots < k_m < k_{m+1} = 1\}$  recursively,

$$b_l^1(x) = \begin{cases} 1, & k_l \leq x < k_{l+1} \\ 0, & \text{otherwise} \end{cases}$$

and

$$b_l^q(x) = \frac{x - k_l}{k_{l+q-1} - k_l} b_l^{q-1}(x) + \frac{k_{l+q} - x}{k_{l+q} - k_{l+1}} b_{l+1}^{q-1}(x). \quad (\text{A1})$$

Then under some smoothness conditions,  $f(x) \approx s(x) = \sum_l b_l^q(x) \beta_l = \mathbf{b}(x)^\top \boldsymbol{\beta}$ , where  $\beta_i \in \mathbb{R}^p$  with  $p = m + q$ . For the random variable  $X$  satisfying Condition 4.11, we have  $\mathbb{E}[b_l^q(X)] \leq C_1 d_n^{-1}$ ,  $\mathbb{E}[b_l^q(X)]^2 \leq C_2 d_n^{-1}$  for some constants  $C_1$  and  $C_2$ . The detailed proofs refer to Stone (1985); Huang et al. (2010); Fan et al. (2011).



Additionally, we restate the result in [Huang et al. \(2010\)](#) for the approximation error rate under B-spline basis function.

**Lemma 6.1** ([Stone \(1985\)](#); [Huang et al. \(2010\)](#)). Suppose Condition [4.11](#) holds and if the number of spline series is chosen by  $d_n = \mathcal{O}(n^{1/(2\kappa+1)})$ . Then there exists an  $f_{jkl}^{d_n} \in \mathcal{S}_n$  satisfying

$$\|f_{jkl}^{d_n} - f_{jkl}^*\|_2^2 = \mathcal{O}_p(d_n^{-2\kappa}) = \mathcal{O}_p(n^{-2\kappa/(2\kappa+1)}). \quad (\text{A2})$$

## A2 Additional conditions for Section [4.1](#)

In this section, we present addition conditions for Lipschitz-gradient (Conditions [6.2-6.3](#)), sparse strongly convex (Conditions [6.4-6.5](#)), and statistical error (Conditions [6.6-6.7](#)) for the update of  $\mathbf{b}_2$  and  $\mathbf{b}_3$ . We define  $\nabla_2\mathcal{L}(\cdot, \cdot, \cdot)$  and  $\nabla_3\mathcal{L}(\cdot, \cdot, \cdot)$  are the gradient taken with respect to the second and the third argument.

**Condition 6.2.** For  $\mathbf{b}_1 \in \mathcal{B}_{\alpha_1, s_1}(\mathbf{b}_1^*)$ ,  $\mathbf{b}_3 \in \mathcal{B}_{\alpha_3, s_3}(\mathbf{b}_3^*)$ , the noiseless gradient function  $\nabla_2\tilde{\mathcal{L}}(\cdot, \mathbf{b}_2^*, \mathbf{b}_3)$  satisfies  $\mu'_{1n}$ -Lipschitz-gradient condition, and  $\nabla_2\tilde{\mathcal{L}}(\mathbf{b}_1^*, \mathbf{b}_2^*, \cdot)$  satisfies  $\mu'_{3n}$ -Lipschitz-gradient condition. That is,

$$\begin{aligned} \langle \nabla_2\tilde{\mathcal{L}}(\mathbf{b}_1, \mathbf{b}_2^*, \mathbf{b}_3) - \nabla_2\tilde{\mathcal{L}}(\mathbf{b}_1^*, \mathbf{b}_2^*, \mathbf{b}_3), \mathbf{b}_2 - \mathbf{b}_2^* \rangle &\leq \mu'_{1n} \|\mathbf{b}_2 - \mathbf{b}_2^*\|_2 \|\mathbf{b}_1 - \mathbf{b}_1^*\|_2 \\ \langle \nabla_2\tilde{\mathcal{L}}(\mathbf{b}_1^*, \mathbf{b}_2^*, \mathbf{b}_3) - \nabla_2\tilde{\mathcal{L}}(\mathbf{b}_1^*, \mathbf{b}_2^*, \mathbf{b}_3^*), \mathbf{b}_2 - \mathbf{b}_2^* \rangle &\leq \mu'_{3n} \|\mathbf{b}_2 - \mathbf{b}_2^*\|_2 \|\mathbf{b}_3 - \mathbf{b}_3^*\|_2, \end{aligned}$$

with probability at least  $1 - \delta_1$ .

**Condition 6.3.** For  $\mathbf{b}_1 \in \mathcal{B}_{\alpha_1, s_1}(\mathbf{b}_1^*)$ ,  $\mathbf{b}_2 \in \mathcal{B}_{\alpha_2, s_2}(\mathbf{b}_2^*)$ , the noiseless gradient function  $\nabla_3\tilde{\mathcal{L}}(\mathbf{b}_1, \cdot, \mathbf{b}_3^*)$  satisfies  $\mu''_{2n}$ -Lipschitz-gradient condition, and  $\nabla_3\tilde{\mathcal{L}}(\cdot, \mathbf{b}_2^*, \mathbf{b}_3^*)$  satisfies  $\mu''_{1n}$ -Lipschitz-gradient condition. That is,

$$\begin{aligned} \langle \nabla_3\tilde{\mathcal{L}}(\mathbf{b}_1, \mathbf{b}_2, \mathbf{b}_3^*) - \nabla_3\tilde{\mathcal{L}}(\mathbf{b}_1, \mathbf{b}_2^*, \mathbf{b}_3^*), \mathbf{b}_3 - \mathbf{b}_3^* \rangle &\leq \mu''_{2n} \|\mathbf{b}_3 - \mathbf{b}_3^*\|_2 \|\mathbf{b}_2 - \mathbf{b}_2^*\|_2 \\ \langle \nabla_3\tilde{\mathcal{L}}(\mathbf{b}_1, \mathbf{b}_2^*, \mathbf{b}_3^*) - \nabla_3\tilde{\mathcal{L}}(\mathbf{b}_1^*, \mathbf{b}_2^*, \mathbf{b}_3^*), \mathbf{b}_3 - \mathbf{b}_3^* \rangle &\leq \mu''_{1n} \|\mathbf{b}_3 - \mathbf{b}_3^*\|_2 \|\mathbf{b}_1 - \mathbf{b}_1^*\|_2, \end{aligned}$$

with probability at least  $1 - \delta_1$ .

**Condition 6.4.** For any  $\mathbf{b}_1 \in \mathcal{B}_{\alpha_1, s_1}(\mathbf{b}_1^*)$ ,  $\mathbf{b}_3 \in \mathcal{B}_{\alpha_3, s_3}(\mathbf{b}_3^*)$ , the loss function  $\mathcal{L}(\cdot, \cdot, \cdot)$  is sparse strongly convex in its first variable, namely

$$\mathcal{L}(\mathbf{b}_1, \mathbf{b}_2^*, \mathbf{b}_3) - \mathcal{L}(\mathbf{b}_1, \mathbf{b}_2, \mathbf{b}_3) - \langle \nabla_2\mathcal{L}(\mathbf{b}_1, \mathbf{b}_2^*, \mathbf{b}_3), \mathbf{b}_2^* - \mathbf{b}_2 \rangle \geq \frac{\gamma_{2n}}{2} \|\mathbf{b}_2 - \mathbf{b}_2^*\|_2^2,$$

with probability at least  $1 - \delta_2$ . Here,  $\gamma_{2n} > 0$  is the strongly convex parameter.

**Condition 6.5.** For any  $\mathbf{b}_1 \in \mathcal{B}_{\alpha_1, s_1}(\mathbf{b}_1^*)$ ,  $\mathbf{b}_2 \in \mathcal{B}_{\alpha_2, s_2}(\mathbf{b}_2^*)$ , the loss function  $\mathcal{L}(\cdot, \cdot, \cdot)$  is sparse strongly convex in its first variable, namely

$$\mathcal{L}(\mathbf{b}_1, \mathbf{b}_2, \mathbf{b}_3^*) - \mathcal{L}(\mathbf{b}_1, \mathbf{b}_2, \mathbf{b}_3) - \langle \nabla_3 \mathcal{L}(\mathbf{b}_1, \mathbf{b}_2, \mathbf{b}_3^*), \mathbf{b}_3 - \mathbf{b}_3^* \rangle \geq \frac{\gamma_{3n}}{2} \|\mathbf{b}_3 - \mathbf{b}_3^*\|_2^2,$$

with probability at least  $1 - \delta_2$ . Here,  $\gamma_{3n} > 0$  is the strongly convex parameter.

**Condition 6.6.** For any  $\mathbf{b}_1 \in \mathcal{B}_{\alpha_1, s_1}(\mathbf{b}_1^*)$ ,  $\mathbf{b}_3 \in \mathcal{B}_{\alpha_3, s_3}(\mathbf{b}_3^*)$ , we have with probability at least  $1 - \delta_3$ ,

$$\|\nabla_2 \mathcal{L}(\mathbf{b}_1, \mathbf{b}_2^*, \mathbf{b}_3) - \nabla_2 \tilde{\mathcal{L}}(\mathbf{b}_1, \mathbf{b}_2^*, \mathbf{b}_3)\|_{\mathcal{P}^*} \leq \varepsilon_2.$$

**Condition 6.7.** For any  $\mathbf{b}_1 \in \mathcal{B}_{\alpha_1, s_1}(\mathbf{b}_1^*)$ ,  $\mathbf{b}_2 \in \mathcal{B}_{\alpha_2, s_2}(\mathbf{b}_2^*)$ , we have with probability at least  $1 - \delta_3$ ,

$$\|\nabla_3 \mathcal{L}(\mathbf{b}_1, \mathbf{b}_2, \mathbf{b}_3^*) - \nabla_3 \tilde{\mathcal{L}}(\mathbf{b}_1, \mathbf{b}_2, \mathbf{b}_3^*)\|_{\mathcal{P}^*} \leq \varepsilon_3.$$

## References

- ANANDKUMAR, A., GE, R., HSU, D., KAKADE, S. M. and TELGARSKY, M. (2014). Tensor decompositions for learning latent variable models. *Journal of Machine Learning Research* **15** 2773–2832.
- BALAKRISHNAN, S., WAINWRIGHT, M. J., YU, B. ET AL. (2017). Statistical guarantees for the em algorithm: From population to sample-based analysis. *The Annals of Statistics* **45** 77–120.
- CHI, E. C. and KOLDA, T. G. (2012). On tensors, sparsity, and nonnegative factorizations. *SIAM Journal on Matrix Analysis and Applications* **33** 1272–1299.
- CHOI, Y., FONTOURA, M., GABRILOVICH, E., JOSIFOVSKI, V., MEDIANO, M. and PANG, B. (2010). Using landing pages for sponsored search ad selection. In *WWW*.
- FAN, J., FENG, Y. and SONG, R. (2011). Nonparametric independence screening in sparse ultra-high-dimensional additive models. *Journal of the American Statistical Association* **106** 544–557.
- GUHANIYOGI, R., QAMAR, S. and DUNSON, D. B. (2017). Bayesian tensor regression. *The Journal of Machine Learning Research* **18** 2733–2763.
- GUO, W., KOTSIA, I. and PATRAS, I. (2012). Tensor learning for regression. *IEEE Transactions on Image Processing* **21** 816–827.

- HAO, B., SUN, W. W., LIU, Y. and CHENG, G. (2017). Simultaneous clustering and estimation of heterogeneous graphical models. *The Journal of Machine Learning Research* **18** 7981–8038.
- HAO, B., ZHANG, A. and CHENG, G. (2018). Sparse and low-rank tensor estimation via cubic sketchings. *arXiv preprint arXiv:1801.09326* .
- HOFF, P. D. (2015). Multilinear tensor regression for longitudinal relational data. *The Annals of Applied Statistics* **9** 1169.
- HUANG, J., HOROWITZ, J. L. and WEI, F. (2010). Variable selection in nonparametric additive models. *Annals of statistics* **38** 2282.
- HUNG, H. and WANG, C.-C. (2012). Matrix variate logistic regression model with application to eeg data. *Biostatistics* **14** 189–202.
- KANAGAWA, H., SUZUKI, T., KOBAYASHI, H., SHIMIZU, N. and TAGAMI, Y. (2016). Gaussian process nonparametric tensor estimator and its minimax optimality. In *International Conference on Machine Learning*.
- KOLDA, T. and BADER, B. (2009). Tensor decompositions and applications. *SIAM Review* **51** 455–500.
- LI, B., KIM, M. K., ALTMAN, N. ET AL. (2010). On dimension folding of matrix-or array-valued statistical objects. *The Annals of Statistics* **38** 1094–1121.
- LI, L. and ZHANG, X. (2017). Parsimonious tensor response regression. *Journal of the American Statistical Association* **112** 1131–1146.
- MA, C., WANG, K., CHI, Y. and CHEN, Y. (2017). Implicit regularization in nonconvex statistical estimation: Gradient descent converges linearly for phase retrieval, matrix completion and blind deconvolution. *arXiv preprint arXiv:1711.10467* .
- MEIER, L., VAN DE GEER, S., BÜHLMANN, P. ET AL. (2009). High-dimensional additive modeling. *The Annals of Statistics* **37** 3779–3821.
- NEGAHBAN, S. and WAINWRIGHT, M. (2011). Estimation of (near) low-rank matrices with noise and high-dimensional scaling. *Annals of Statistics* **39** 1069–1097.
- NEGAHBAN, S. N., RAVIKUMAR, P., WAINWRIGHT, M. J. and YU, B. (2012). A unified framework for high-dimensional analysis of  $m$ -estimators with decomposable regularizers. *Statist. Sci.* **27** 538–557.

- PARK, S.-T. and CHU, W. (2009). Pairwise preference regression for cold-start recommendation. In *Proceedings of the third ACM conference on Recommender systems*. ACM.
- RABUSSEAU, G. and KADRI, H. (2016). Low-rank regression with tensor responses. In *Advances in Neural Information Processing Systems*.
- RASKUTTI, G., YUAN, M. and CHEN, H. (2019). Convex regularization for high-dimensional multiresponse tensor regression. *Annals of Statistics* **47** 1554–1584.
- RAVIKUMAR, P., LAFFERTY, J., LIU, H. and WASSERMAN, L. (2009). Sparse additive models. *Journal of the Royal Statistical Society: Series B (Statistical Methodology)* **71** 1009–1030.
- STONE, C. J. (1985). Additive regression and other nonparametric models. *The Annals of Statistics* 689–705.
- SUN, W. W. and LI, L. (2017). Store: sparse tensor response regression and neuroimaging analysis. *The Journal of Machine Learning Research* **18** 4908–4944.
- SUN, W. W. and LI, L. (2018). Dynamic tensor clustering. *Journal of the American Statistical Association* 1–30.
- SUN, W. W., LU, J., LIU, H. and CHENG, G. (2017). Provable sparse tensor decomposition. *Journal of the Royal Statistical Society: Series B (Statistical Methodology)* **79** 899–916.
- SUZUKI, T., KANAGAWA, H., KOBAYASHI, H., SHIMIZU, N. and TAGAMI, Y. (2016). Minimax optimal alternating minimization for kernel nonparametric tensor learning. In *Advances in Neural Information Processing Systems*.
- WAINWRIGHT, M. J. (2014). Structured regularizers for high-dimensional problems: Statistical and computational issues. *Annual Review of Statistics and Its Application* **1** 233–253.
- WANG, Z., LIU, H. and ZHANG, T. (2014). Optimal computational and statistical rates of convergence for sparse nonconvex learning problems. *Annals of statistics* **42** 2164.
- XU, J., SHAO, X., MA, J., CHIH LEE, K., QI, H. and LU, Q. (2016). Lift-based bidding in ad selection. In *AAAI*.
- YI, X. and CARAMANIS, C. (2015). Regularized em algorithms: A unified framework and statistical guarantees. In *Advances in Neural Information Processing Systems*.

- YU, R. and LIU, Y. (2016). Learning from multiway data: Simple and efficient tensor regression. In *International Conference on Machine Learning*.
- YUAN, M. and LIN, Y. (2006). Model selection and estimation in regression with grouped variables. *Journal of the Royal Statistical Society: Series B* **68** 49–67.
- YUAN, M. and ZHANG, C. (2016). On tensor completion via nuclear norm minimization. *Foundations of Computational Mathematics* **16** 1031–1068.
- ZHANG, A. (2019). Cross: Efficient low-rank tensor completion. *Annals of Statistics* To Appear.
- ZHANG, A. and HAN, R. (2019). Optimal sparse singular value decomposition for high-dimensional high-order data. *Journal of the American Statistical Association* To Appear.
- ZHE, S., ZHANG, K., WANG, P., CHIH LEE, K., XU, Z., QI, Y. and GHAHRAMANI, Z. (2016). Distributed flexible nonlinear tensor factorization. In *Advances in Neural Information Processing Systems*.
- ZHOU, H., LI, L. and ZHU, H. (2013). Tensor regression with applications in neuroimaging data analysis. *Journal of the American Statistical Association* **108** 540–552.
- ZHU, H., CHEN, Y., IBRAHIM, J. G., LI, Y., HALL, C. and LIN, W. (2009). Intrinsic regression models for positive-definite matrices with applications to diffusion tensor imaging. *Journal of the American Statistical Association* **104** 1203–1212.